Atmos. Chem. Phys., 15, 13615–13625, 2015
www.atmos-chem-phys.net/15/13615/2015/
doi:10.5194/acp-15-13615-2015

Atmospheric Chemistry and Physics
Open Access
EGU

Viscosity controls humidity dependence of N_2O_5 uptake to citric acid aerosol

G. Gržinić[1,2], T. Bartels-Rausch[1], T. Berkemeier[3], A. Türler[1,2], and M. Ammann[2]

[1]Laboratory of Radiochemistry and Environmental Chemistry, Paul Scherrer Institute, 5232 Villigen, Switzerland
[2]Department of Chemistry and Biochemistry, University of Bern, 3012 Bern, Switzerland
[3]Multiphase Chemistry Department, Max Planck Institute for Chemistry, 55128 Mainz, Germany

Correspondence to: M. Ammann (markus.ammann@psi.ch)

Received: 2 July 2015 – Published in Atmos. Chem. Phys. Discuss.: 14 August 2015
Revised: 12 November 2015 – Accepted: 23 November 2015 – Published: 9 December 2015

Abstract. The heterogeneous loss of dinitrogen pentoxide (N_2O_5) to aerosol particles has a significant impact on the night-time nitrogen oxide cycle and therefore the oxidative capacity in the troposphere. Using a ^{13}N short-lived radioactive tracer method, we studied the uptake kinetics of N_2O_5 on citric acid aerosol particles as a function of relative humidity (RH). The results show that citric acid exhibits lower reactivity than similar dicarboxylic and polycarboxylic acids, with uptake coefficients between $\sim 3\times10^{-4}$–$\sim 3\times10^{-3}$ depending on humidity (17–70 % RH). At RH above 50 %, the magnitude and the humidity dependence can be best explained by the viscosity of citric acid as compared to aqueous solutions of simpler organic and inorganic solutes and the variation of viscosity with RH and, hence, diffusivity in the organic matrix. Since the diffusion rates of N_2O_5 in highly concentrated citric acid solutions are not well established, we present four different parameterizations of N_2O_5 diffusivity based on the available literature data or estimates for viscosity and diffusivity of H_2O. Above 50 % RH, uptake is consistent with the reacto-diffusive kinetic regime whereas below 50 % RH, the uptake coefficient is higher than expected from hydrolysis of N_2O_5 within the bulk of the particles, and the uptake kinetics is most likely limited by loss on the surface only. This study demonstrates the impact of viscosity in highly oxidized and highly functionalized secondary organic aerosol material on the heterogeneous chemistry of N_2O_5 and may explain some of the unexpectedly low loss rates to aerosol derived from field studies.

1 Introduction

Dinitrogen pentoxide (N_2O_5) is an important species of night-time atmospheric chemistry (Abbatt et al., 2012; Chang et al., 2011; Dentener and Crutzen, 1993). Nitrogen dioxide (NO_2) reacts with ozone (O_3) to give the nitrate radical (NO_3). N_2O_5 is formed via Reaction (R1).

$$NO_3 + NO_2 + M \rightleftarrows N_2O_5 + M \quad \text{(R1)}$$

The concentrations of N_2O_5, NO_3 and NO_2 are controlled by the temperature-dependent equilibrium (Reaction R1). N_2O_5 hydrolyzes on any humid surface or in aqueous solution, to give HNO_3 (Rection R2).

$$N_2O_5 + H_2O \longrightarrow 2HNO_3 \quad \text{(R2)}$$

In Reaction (R2), which is considered unimportant in the gas phase, H_2O represents either adsorbed water, ice or liquid water, present on ground or on airborne particles. The detailed mechanism behind Reaction (R2) that drives heterogeneous uptake of N_2O_5 on aerosol particles is complex (Hallquist et al., 2003; Mozurkewich and Calvert, 1988; Wahner et al., 1998). The suggested elementary steps of the mechanism are the following:

$$N_2O_{5(g)} \longrightarrow N_2O_{5(aq)} \quad \text{(R3)}$$
$$N_2O_{5(aq)} \longrightarrow N_2O_{5(g)} \quad \text{(R4)}$$
$$N_2O_{5(aq)} \longrightarrow NO^+_{2(aq)} + NO^-_{3(aq)} \quad \text{(R5)}$$
$$NO^+_{2(aq)} + NO^-_{3(aq)} \longrightarrow N_2O_{5(aq)} \quad \text{(R6)}$$
$$NO^+_{2(aq)} + H_2O_{(liq)} \longrightarrow HNO_{3(aq)} + H^+_{(aq)}. \quad \text{(R7)}$$

A reversible disproportionation (Reactions R5, R6) precedes the actual reaction of the nitronium ion NO_2^+ with water (Reaction R7). In case of nitrate already present in the particle phase, uptake is considerably reduced through Reaction (R6), referred to as the nitrate effect (Mentel et al., 1999). The aqueous HNO_3 formed in Reaction (R7) can either deprotonate to yield nitrate or evaporate from the particle according to its volatility and acid–base chemistry with other solutes in the system (Laskin et al., 2012). Water plays an important role in the mechanism, not only for solvation of N_2O_5 (Reactions R3, R4) and hydration of the nitronium ion, but it is also the main reaction partner of the nitronium ion in absence of other nucleophiles (such as chloride, which are not considered in this work).

Heterogeneous hydrolysis of N_2O_5 on aerosols acts as a sink for atmospheric NO_x species, and has therefore a significant impact on ozone production and the oxidative capacity of the atmosphere (Dentener and Crutzen, 1993). N_2O_5 uptake kinetics on aerosols has thus received substantial interest over the past decades (Abbatt et al., 2012). The loss rate of N_2O_5 from the gas phase to aerosol particles is expressed in terms of the uptake coefficient, γ, which represents the probability that a gas kinetic collision of a N_2O_5 molecule leads to its uptake at the interface. Extensive studies on inorganic aerosols or corresponding proxy systems have shown that the primary factors influencing the uptake coefficient in the range of 0.0001 to 0.05 are relative humidity (RH), physical state, particle size, and composition (Abbatt et al., 2012; Davis et al., 2008; George et al., 1994; Hallquist et al., 2003; Hanson and Ravishankara, 1991; Hu and Abbatt, 1997; Karagulian et al., 2006; Mozurkewich and Calvert, 1988; Vandoren et al., 1991; Wahner et al., 1998). Supersaturated liquid particles have shown uptake coefficients up to 1–2 orders of magnitude higher than corresponding solid particles at the same RH, pointing towards the importance of the hydrolysis reaction (Reactions R3–R7) of N_2O_5 with liquid water present in the bulk of aerosol particles (Hallquist et al., 2003; Thornton and Abbatt, 2005).

Recently, the focus of N_2O_5 uptake studies has shifted towards organic and mixed inorganic and organic aerosol particles (Anttila et al., 2006; Gaston et al., 2014; Griffiths et al., 2009; Gross et al., 2009; Thornton et al., 2003). Hydrophobic organics may rather form organic surface films or phase separated liquid coatings and thereby may suppress γ for N_2O_5 significantly compared to pure inorganic aerosols (Badger et al., 2006; Riemer et al., 2009; Thornton and Abbatt, 2005). In turn, particles composed of hygroscopic organics, such as polycarboxylic acids, show uptake coefficient values that in some cases approach those for inorganic aerosols due to their high water content (Griffiths et al., 2009; Thornton et al., 2003), and the humidity-dependent uptake can be understood in terms of the activity of water as reactant (Bertram and Thornton, 2009; Ammann et al., 2013).

Organic aerosols account for a significant fraction of atmospheric particulate mass (Kanakidou et al., 2005). However there are still significant gaps in our knowledge regarding the chemistry and physical state of organic aerosols (De Gouw and Jimenez, 2009; Kanakidou et al., 2005; Zhang et al., 2007). Recent studies have shown that the previous assumptions of low-viscosity, well-mixed liquid aerosol phases are not always correct, but must be considered depending on environmental conditions such as humidity and temperature. Especially under cold or dry conditions, aerosol particles dominated by organic compounds can exhibit a highly viscous or even glassy state (Koop et al., 2011; Murray, 2008; Renbaum-Wolff et al., 2013; Virtanen et al., 2010; Zobrist et al., 2008). Diffusion in these particles is significantly retarded (Price et al., 2014; Zobrist et al., 2011), leading to severe kinetic limitations in gas-particle partitioning (Shiraiwa et al., 2013; Vaden et al., 2011).

Field measurements (Bertram et al., 2009; Brown et al., 2009) have shown that the observed reactivity of N_2O_5 on aerosol particles containing organics can be up to a factor of 10 lower than the values predicted by model parameterizations, which are based on laboratory measurements with organic compounds such as malonic acid. Also, a recent laboratory study has shown that uptake of N_2O_5 to laboratory SOA proxies does not follow exclusively the expected trend with water content based on the correlation of the latter with O : C ratio (Gaston et al., 2014).

For this study we investigated the uptake of N_2O_5 on citric acid aerosol using the short-lived ^{13}N radioactive tracer technique developed at the Paul Scherrer Institute (Ammann, 2001; Gržinić et al., 2014). This technique has been used before to study the uptake kinetics of other nitrogen oxides on aerosol particles (Guimbaud et al., 2002; Sosedova et al., 2009; Vlasenko et al., 2009), and we have recently developed a method to produce ^{13}N-labelled N_2O_5 for this purpose (Gržinić et al., 2014). Citric acid was used as a proxy for highly oxidized organic species found in secondary organic aerosol (SOA). It has well-known thermodynamic properties and new studies on viscosity and water diffusivity in citric acid have recently become available (Lienhard et al., 2012, 2014). In our study, measurements were conducted over a wide RH range, and several methods were used to estimate the diffusivity of N_2O_5 in citric acid as a basis for the kinetic analysis.

2 Experimental

The experimental method used in this study has been described in detail in our previous publication (Gržinić et al., 2014). N_2O_5 labelled with the ^{13}N short-lived radioactive isotope is mixed with citric acid aerosol in an aerosol flow tube. Gas and aerosol phase products are selectively separated and trapped in a parallel plate diffusion denuder system and a particle filter, respectively. The concentration of the various species can be measured simultaneously by monitoring the radioactive decay of the ^{13}N-labelled species on each

trap over time. A schematic representation of our experimental setup can be found in Gržinić et al. (2014).

2.1 Production of ^{13}N-labelled N_2O_5

^{13}N ($\tau_{1/2} \approx 10$ min) is produced online in a flow-through gas-target via the $^{16}O(p,\alpha)^{13}N$ reaction in 10–15 % O_2 in He, at a total flow rate of 1 standard L min^{-1} at ~ 2 bar (see Ammann, 2001; Gržinić et al., 2014, for more details). The highly oxidized ^{13}N-labelled nitrogen species, are reduced to ^{13}NO over a Mo converter (at ~ 380 °C) and transported from the production site to the laboratory through a 580 m long 4 mm inner diameter polyvinylidene fluoride (PVDF) tube. A small amount of the ^{13}NO containing gas flow (50 mL min^{-1}) is mixed with nitrogen carrier gas and non-labelled NO (~ 2 mL min^{-1}) from a certified gas cylinder (10 ppm in N_2). O_3 at ~ 8 ppmv is produced by irradiating a flow (50 mL min^{-1}) of 10 % O_2 in N_2 with 185 nm UV light in a cylindrical photolysis reactor. The ^{13}NO and O_3 flows are mixed in the N_2O_5 synthesis reactor (34 cm long and 4 cm inner diameter, with residence time ~ 4 min), where NO reacts with O_3 to produce first NO_2 and then NO_3, which then react via Reaction (R1) to form N_2O_5. This reactor is covered inside with a thin polytetrafluoroethylene (PTFE) foil to minimize heterogeneous N_2O_5 losses, and outside by a dark cloth shroud to prevent NO_3 photolysis. Design, performance and consistency of N_2O_5 production with simulations obtained via a gas kinetic model has been described previously (Gržinić et al., 2014).

2.2 Aerosol production

An ultrasonic nebulizer was used to generate an aerosol from a 0.07 % (by weight) solution of citric acid (HQ, Fluka, > 99 %) in MilliQ water. The resulting aerosol particles were dried over a Nafion membrane diffusion drier. Citric acid particles remain in liquid (supersaturated) form over a very wide humidity range (6–90 % RH) and neither crystallization (efflorescence) nor deliquescence has been reported over this range (Peng et al., 2001; Zardini et al., 2008). To avoid possible efflorescence of the aerosol particles in dry air, the sheath gas used in the diffusion drier has been humidified to 15–17 % RH. The resulting aerosol gas flow was passed through a homemade ^{85}Kr bipolar ion source to establish an equilibrium charge distribution on the aerosol, followed by an electrostatic precipitator to remove all charged particles. This was done to avoid uncontrollable wall losses of charged particles in the insulating aerosol flow tube. A homemade Gore-Tex™ membrane humidifier was placed behind the precipitator for precise adjustment of RH, followed by an elution volume with ~ 2 min residence time to assure gas – particle equilibrium. Measurements were conducted from 17 to 70.3 % RH.

A Scanning Mobility Particle Sizer (SMPS) was used to measure the suspended surface area to gas volume ratio. The SMPS system consisted of an ^{85}Kr ion source (to re-establish the equilibrium charge distribution), a Differential Mobility Analyzer (DMA, TSI 3071) and a Condensation Particle Counter (CPC, TSI 3022). Filtered carrier gas was used as sheath gas for the DMA to assure identical RH in the two flows and thus maintain the water content of the particles during size separation. The SMPS was connected immediately after the aerosol flow tube. A capacitance humidity sensor was placed in front of the SMPS to monitor RH.

2.3 Aerosol flow tube

The gas flows containing aerosol and N_2O_5, respectively, were mixed in a cylindrical flow tube reactor consisting of a perfluoroalkoxy copolymer (PFA) tube with an inner diameter of 7 cm. The inlet and outlet are cylindrical PTFE stops with inverse cones milled into. The stops are equipped with a pneumatic ring to seal the reactor. The inlet and outlet can be moved inside the reactor to vary reaction time. The N_2O_5 gas flow (102 mL min^{-1}) is introduced into the aerosol flow tube along the axis of the reactor. The distance between the N_2O_5 reactor and the aerosol flow tube was kept short, and the N_2O_5 reactor was moved along with the inlet into the aerosol flow tube when changing the reaction time. The aerosol flow (720 mL min^{-1}) is introduced via a stainless-steel tubular injector (6 mm in diameter) which protrudes from the inlet and is bent in such a way that the injector nozzle is equidistant from the walls of the flow tube. The aerosol flow is injected perpendicularly to the N_2O_5 gas flow within the flow tube. Reaction times from 10 to 60 s were adjusted. For the flow rate used, a laminar flow profile is assumed to have been established within the flow tube a few cm downstream of the aerosol injector. As with the N_2O_5 synthesis reactor, a black shroud was used to shield the aerosol flow tube from daylight to prevent NO_3 photolysis and thus loss of N_2O_5. The overall system exhaust was pressure controlled at slightly below ambient pressure (960–970 mbar). The aerosol flow tube was kept at ambient temperature, which was controlled by the room ventilation system at 295 ± 1 K.

2.4 Separation and detection of ^{13}N-labelled species

The gas flow from the aerosol flow tube was split with one fraction going to the SMPS system or alternatively a NO_x (Teledyne T200) or O_3 analyzer (ML 9810) and the other being directed into the parallel plate diffusion denuder system. This system consists of a series of parallel plate sets placed 1 mm apart in an aluminium housing. The plates are prepared with specific coatings and trap the ^{13}N containing gaseous species (N_2O_5, NO_3 and NO_2) by lateral diffusion and chemical reaction. Aerosol particles pass through the denuder without being trapped and are deposited on a glass fiber filter located at the exit of the denuder system. Citric acid has been used as a denuder coating for N_2O_5. Citric acid mixes well with water, has a well-known hygroscopic cycle

(Peng et al., 2001; Zardini et al., 2008), and interferes only weakly with NO_2; i.e. only marginal amounts are trapped on the denuder plates. Citric acid was used as a coating on the first two denuder plates, the first one capturing N_2O_5, while the second one is used to quantify the small NO_2 interference. NO_3, which is present in small quantities in the gas phase, cannot be separated from N_2O_5 by this technique and is likewise absorbed on the first denuder plate together with N_2O_5. The citric acid coating was prepared by applying a citric acid solution 2 % by weight in 50 / 50 % methanol / water to the plates and allowed to dry at room temperature. The following two denuders were coated with a 1 % N-(1-naphtyl) ethylene diamine dihydrochloride (NDA) solution in 1 % KOH and 10 % water in methanol. NDA reacts efficiently with NO_2 and the basic nature of the solution prevents the re-evaporation of the so formed nitrite. Since NDA is sensitive to O_3, which is present at around ~ 550 ppbv in our system, two sets of denuder plates were installed in series to extend the operating life. Fresh coatings were prepared and applied every day. An additional gamma detector was attached to the non-coated, 10 cm long, and trapezoidally shaped aluminium inlet to determine the amount of N_2O_5 trapped there.

The ^{13}N containing species that were trapped on the denuder plates, inlet and particle filter were measured by monitoring the radioactive decay of ^{13}N. A CsI scintillator crystal with integrated PIN diode detector (Carroll and Ramsey, USA) was placed on each of the traps. ^{13}N, a well-known β^+ emitter, decays with emission of a positron which, upon annihilation with an electron, emits two coincident γ-rays in opposite directions. These γ-rays are detected by the scintillators and the signal is converted to the flux of the ^{13}N containing gaseous species into the respective traps using the inversion procedure reported elsewhere (Kalberer et al., 1996). The flux into a trap can be calculated using Eq. (1):

$$I_j = \frac{A_{j(i)} - A_{j(i-1)} \exp(-\lambda(t_{(i)} - t_{(i-1)}))}{1 - \exp(-\lambda(t_{(i)} - t_{(i-1)}))}, \quad (1)$$

where I_j is the flux into trap j, $A_{j(i-1)}$ and $A_{j(i)}$ are two consecutive activity measurements performed at times $t_{(i-1)}$ and $t_{(i)}$, and λ is the decay constant for ^{13}N ($\lambda = 0.00116\,s^{-1}$). The measured flux is proportional to the gas phase concentration of the respective species. By comparing the value of the gas phase NO_2 concentration measured with the NO_x analyzer to the $^{13}NO_2$ and $^{13}N_2O_5$ signals measured at the denuder traps and the particle filter, it is possible to calculate the concentration of N_2O_5 in the gas phase and its degradation products in the particle phase. The overall signal of N_2O_5 in the gas phase was obtained by adding the inlet and first citric acid coated denuder plate signals and subtracting the second citric acid denuder signal (NO_2 interference). To correct for the small amounts of NO_3 present in the gas phase the signal was multiplied with the $N_2O_5/(NO_3+N_2O_5)$ ratio obtained via the gas kinetic model described in our previous study (Gržinić et al., 2014).

Additional information on coating preparation, traps and measurement efficiencies can be found in our previous publications (Ammann, 2001; Gržinić et al., 2014; Guimbaud et al., 2002).

3 Results and discussion

3.1 Uptake coefficient of N_2O_5 as a function of relative humidity

A typical experiment was performed as follows: after a period of stabilization, during which all flows were switched on, but the nebulizer switched off, the NO and NO_2 concentrations were measured via the NO_x analyzer connected to the system (in place of the SMPS), before turning on the O_3 generator. Concentrations around 9–10 ppbv of NO were obtained in the aerosol flow tube reactor. From the measured gamma-ray detector signals of N_2O_5 and NO_2, after switching on the O_3 generator, typically, a maximum initial concentration of ~ 5 ppbv of N_2O_5 was calculated. Next, a wall loss measurement was performed by changing the length of the aerosol flow tube and thus the reaction time, which is shown in the first part of the exemplary record of an experiment in Fig. 1. Typical pseudo-first order wall loss rate constants, k_w, were $\sim 9\times10^{-3}$ and $\sim 3\times10^{-2}\,s^{-1}$ for low and high humidity, respectively, indicating strong wall loss of the labelled N_2O_5 molecules. k_w was remaining constant over time after an initial passivation period. After the wall loss measurement was completed, the SMPS was connected to the system and the reactor length was adjusted to enable a 60 s reaction time within the aerosol flow tube. The wall loss measurement was routinely performed for each set of aerosol experiment.

At this point the nebulizer was switched on to generate citric acid aerosol for 25–30 min and then switched off again for an interval of the same duration. The aerosol surface area was varied by changing the vibration frequency of the piezoelectric membrane in the ultrasonic nebulizer, leading to data as shown in Fig. 2.

The gas-aerosol interaction kinetics can be described by Eq. (2):

$$\frac{C_p^{(t)}}{C_g^{(t=0)}} = \frac{1 - e^{-(k_w+k_p)t}}{1 + \frac{k_w}{k_p}}, \quad (2)$$

where $C_g^{(t=0)}$ is the gas-phase N_2O_5 concentration at time zero, $C_p^{(t)}$ is the N_2O_5 concentration in the particle phase at the end of the reactor, $t = 60$ s, k_w is the wall loss rate constant, measured as described above, and k_p denotes the apparent first order rate coefficient for loss of N_2O_5 from the gas phase due to its heterogeneous reaction with the aerosol phase. Equation (3) relates k_p to the uptake coefficient, γ:

$$\gamma = \frac{4k_p}{S_p\omega} \quad \varpi = \sqrt{\frac{8RT}{\pi M}}, \quad (3)$$

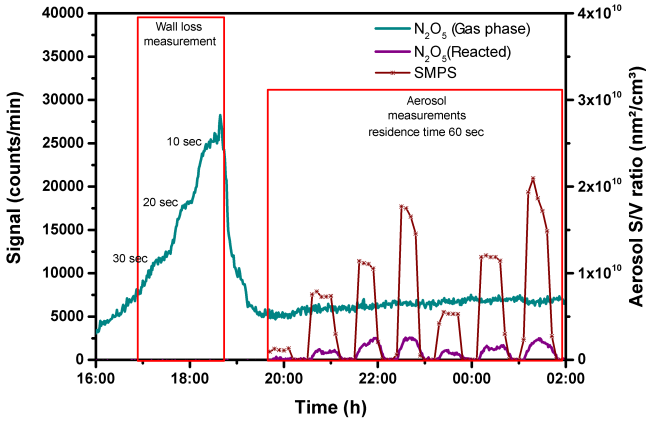

Figure 1. Exemplary traces of inverted detector signals for an experiment: teal: gas-phase $^{13}N_2O_5$ signal; purple: particle-phase ^{13}N signal; red: SMPS signal (aerosol surface / volume ratio).

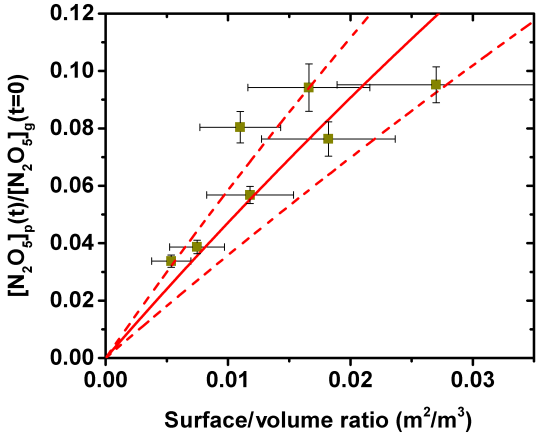

Figure 2. Normalized particle-phase N_2O_5 concentration vs. aerosol surface area to gas volume ratio for the experiment from Fig. 1. The data points represent experimental data; vertical error bars represent a 95 % confidence interval, horizontal error bars represent the S/V measurement error (30 %), the full red line is the fitted series determined by least-squares fitting of Eq. (2) to experimental data, the dashed red lines are 95 % confidence intervals.

where S_p is the total aerosol surface area to gas volume ratio obtained with the SMPS, ω is the mean thermal velocity of N_2O_5, R is the gas constant, T is the absolute temperature and M is the molar weight of N_2O_5. Equation (2) was then used to fit the experimental data as shown in Fig. 2 with γ being the only variable. Note that this procedure of varying the aerosol surface area to volume ratio gave better reproducibility and lower scatter than varying the interaction time. The resulting γ values ranged from 3×10^{-4} to $\sim 3 \times 10^{-3}$ over the RH range of 17 to 70 % as shown in Fig. 3.

The uncertainty in γ arises primarily from the fact that aerosol uptake rates (k_p) were smaller than wall loss rates (k_w) as well as from the systematic error associated with the measurements of surface to volume ratio of the aerosol by the

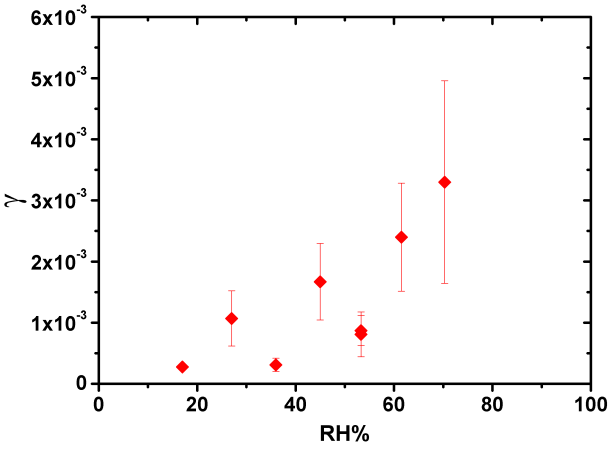

Figure 3. Uptake coefficient of N_2O_5 on citric acid as a function of RH. Error bars represent 95 % confidence bounds. The measured values can be found in Table S1 of the Supplement.

SMPS (S_p), which amounts to ~ 30 %. The 95 % confidence interval from replication (as can be seen in Fig. 2) does not strongly influence the overall uncertainty for γ. There are a few factors that may have influenced the scatter among the measurements at different RH. We have noticed that a small but variable number of very large particles fell outside the measurement range of the DMA, which for our settings was limited to particle diameters up to 806 nm. Additionally, two separate batches of citric acid (from the same manufacturer) have been used to prepare the solutions, and possible contaminations, which might induce phase separation or crystallization, may have affected the physical properties and reactivity of the resulting aerosol.

Compared to other aqueous polycarboxylic acids (Griffiths et al., 2009; Thornton et al., 2003) the uptake coefficient on citric acid is more than an order of magnitude lower. As mentioned in the experimental section, care was taken to avoid crystallization by using a humidified gas flow to equilibrate the solution droplets resulting from the nebulizer to the lowest RH used in the experiments. Therefore, the low uptake coefficients are unlikely to represent uptake to crystalline citric acid. With respect to the humidity range, the primary limitations were wall loss (at high RH) and potential efflorescence of the aqueous aerosol (at RH at or below 6 %, Peng et al., 2001).

As a consistency test we measured the uptake coefficient of N_2O_5 on deliquesced ammonium sulfate aerosol at 52 % RH as described by (Gržinić et al., 2014) and obtained an average value of $(1.4 \pm 0.4) \times 10^{-2}$, similar to other studies compiled by Ammann et al. (2013).

3.2 Physical state, reaction mechanism, and parameterization

The data in Fig. 3 show a gradual increase of the uptake coefficient with increasing RH, consistent with the expected increase in water content. Literature data suggest that citric acid particles form supersaturated solutions down to low RH (Peng et al., 2001; Zardini et al., 2008). Recent experiments have demonstrated high viscosity of highly supersaturated citric acid solutions, obtained either from the kinetics of shape change of coalescing droplets (J. Reid and C. Cai, personal communication, 2015, and using the method described by Power et al., 2013) or via the hygroscopic growth kinetics in single levitated droplets (Lienhard et al., 2014). It is thus not surprising that the observed uptake coefficient of N_2O_5 of around 10^{-4} at low humidity is comparable to succinic acid or oxalic acid in their effloresced (and thus solid) form Griffiths et al. (2009). The difference between low and high humidity is also similar to that of solid (effloresced) vs. liquid (deliquesced) inorganic aerosol (Hallquist et al., 2003), but as mentioned above, the gradual increase observed here is consistent with the absence of a sharp deliquescence step and thus probably the result of continuously changing water content and hence diffusivity of N_2O_5 within the particles. This is in line with previous observations of the gradually changing water content in amorphous organics (Mikhailov et al., 2009).

For moderate uptake rates and submicron particles, where gas-phase diffusion constraints can be neglected, the N_2O_5 uptake coefficient can be described according to the resistor model (Davidovits et al., 1995) with Eq. (4):

$$\frac{1}{\gamma} = \frac{1}{\alpha_b} + \frac{1}{\Gamma_b} = \frac{1}{\alpha_b} + \frac{\omega}{4HRT\sqrt{D_l k^I}}\left(\coth q - \frac{1}{q}\right)^{-1}, \quad (4)$$

where α_b is the bulk accommodation coefficient, H is the Henry's law constant, R is the gas constant, T is the absolute temperature, D_l is the liquid-phase diffusion coefficient, k^I is the apparent first-order loss rate constant for N_2O_5 in the liquid phase, ω is the mean thermal velocity of N_2O_5 molecules in the gas phase and q is the reacto-diffusive parameter which accounts for the competition between reaction and diffusion within the particle. The reacto-diffusive parameter is defined by Eq. (5):

$$q = \frac{l}{r}, \quad (5)$$

where r is the radius of the particle and l is the reacto-diffusive length, defined by Eq. (6):

$$l = \sqrt{\frac{D_l}{k^I}}. \quad (6)$$

The reacto-diffusive length is the characteristic distance that a molecule diffuses within a particle before reacting, which brings about a size dependence of γ when l is comparable to or larger than the radius of the particle ($q > 1$). Equation (5), in which the complex mechanism (Reactions R3–R7) is lumped into the net Reaction (R2) by treating only one dissolved N_2O_5 species undergoing a bimolecular reaction with liquid phase water, provides a reasonable parameterization to describe uptake of N_2O_5 to laboratory generated aerosol particles (Ammann et al., 2013). An analytical expression has been suggested to also take into account the nitrate effect (Griffiths et al., 2009; Bertram and Thornton, 2009). Since we have worked at low N_2O_5 concentrations (5 ppbv), where the maximum HNO_3 concentration expected in the particle phase was $\sim 10^{-3}$ M, we could safely neglect this.

The Henry's law constant for N_2O_5, an important variable in Eq. (4), is unknown for organic polycarboxylic aerosol particles. However, in several studies (Badger et al., 2006; Robinson et al., 1997; Thornton et al., 2003), a generic value of $H = 2\,\mathrm{M\,atm^{-1}}$ has been suggested for liquid aerosol particle solutions. Recommended values (Ammann et al., 2013) for aqueous organic aerosols have been used for α_b (0.035) and k^{II} ($1.0 \times 10^5\,\mathrm{M^{-1}\,s^{-1}}$), which is the apparent second-order rate constant for the reaction of N_2O_5 with water, and $k^I = k^{II}[H_2O]$. The recommended values are based on several studies with dicarboxylic and polycarboxylic acids (Badger et al., 2006; Griffiths et al., 2009; Thornton et al., 2003). Note that as evident from Eq. (4), experiments allow to safely constrain only the product $H \times \sqrt{(k^I)}$, so that the rate constant values are linked to the choice of H.

Since water is the main reactant for the hydrolysis of N_2O_5, the parameterization relies heavily on the water concentration as a function of RH. Mass growth factor values (and consequently mass fractions) for citric acid and water were obtained from Zardini et al. (2008), while the citric acid solution densities have been obtained from several sources, each relating to the particular parameterization used for viscosity further below (Laguerie et al., 1976; Lienhard et al., 2012; Peng et al., 2001).

For the diffusion coefficient D_l of N_2O_5 in an aqueous solution, previous studies were based on an estimate of $1 \times 10^{-5}\,\mathrm{cm^2\,s^{-1}}$ (Badger et al., 2006; Griffiths et al., 2009; Hallquist et al., 2003; Thornton et al., 2003), independent of water activity. Together with the other parameters, this leads to a reasonable agreement of the parameterization based on Eq. (4) with the measured data for malonic acid. However, as it turns out, the parameterization would largely overpredict the reactivity for citric acid. Citric acid solutions exhibit a substantially higher viscosity; i.e. for a solution of 1.04 M, the reported viscosity (Laguerie et al., 1976) of CA is 1.49×10^{-3} Pa s, while for malonic acid it is 1.09×10^{-3} Pa s (Chmielewska and Bald, 2008), close to that of water (0.91×10^{-3} Pa s). It is therefore likely that the lower uptake coefficients of N_2O_5 in citric acid compared to those for malonic acid are caused by lower diffusivity in the

more viscous solution. Since the diffusivity of N_2O_5 is not known in either medium, we used four methods for its estimation, based either on measured viscosities or on measured or estimated diffusivity of H_2O. If the viscosity is known, D_l for N_2O_5 can be calculated by applying the Stokes–Einstein relation (Eq. 7):

$$D_l = \frac{k_B T}{6\pi \eta r}, \quad (7)$$

where k_B is the Boltzmann constant, T is the absolute temperature, η is the viscosity, and r is the radius of the N_2O_5 molecule assumed spherical (2.5 Å). Uncertainty remains with respect to the effective molecular radius to be used, since the identity of the solute for the rate limiting step is not clear (dissolved N_2O_5 or NO_2^+). Additionally, for high viscosity (at low RH), the use of the Stokes–Einstein relation may be questioned: Power et al. (2013) suggested that the diffusivity of water in sucrose droplets decouples from the viscosity at viscosities around 1 Pa s, and at 10 Pa s the diffusivity calculated by Eq. (7) departs from measured values already by an order of magnitude. For the cases, where the diffusivity of H_2O is known or estimated, we also used Eq. (7) to estimate the diffusivity of N_2O_5 by accounting for the change in molecular size.

The results are summarized in Fig. 4. The different parameterizations are represented by solid lines, and by dashed lines where the use of the Stokes–Einstein relation may not be granted. The first one (labelled "Laguerie") is based on viscosity measurements by Laguerie et al. (1976). The viscosity parameterization in this case covers a range of citric acid concentrations up to ~ 4.3 M, which in our case corresponds to RH values > 70 %. More recent measurements of viscosity of citric acid were provided by C. Cai and J. Reid (personal communication, 2015) from a combination of optical tweezers and electrodynamic balance (EDB) experiments covering a range of 3 to 73 % RH (labelled "Reid" in Fig. 4). The third method is based on an estimate of the diffusivity of H_2O in the organic matrix, which is in turn based on the principal parameterization for the one of H_2O in sucrose from Zobrist et al. (2011). This method uses the measured glass transition and hygroscopicity data to infer diffusion properties of a target substance (e.g. citric acid) by extrapolation from a known reference substance (e.g. sucrose) (Berkemeier et al., 2014) (labelled "Berkemeier" in Fig. 4). The same method has been used to estimate the diffusivity of N_2O_5 in malonic acid. Finally, Lienhard et al. (2014) determined the diffusivity of H_2O in citric acid solution droplets by measuring the kinetics of the size change in response to step changes in RH in an EDB. The data are parameterized via an empirical Vignes-type equation (Lienhard et al., 2012, 2014).

The result of calculating the uptake coefficient according to Eq. (4) and using diffusion coefficients estimated according to these four methods is presented in Fig. 5. The solid and dashed shape of the lines again indicate the validity or not, respectively, of the Stokes–Einstein relation as a basis

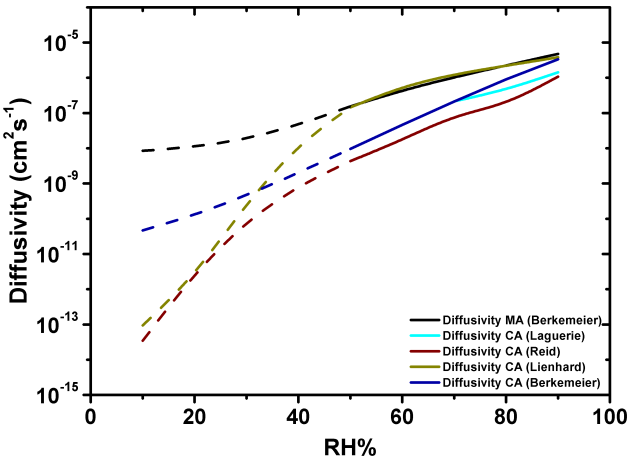

Figure 4. Diffusivity of N_2O_5 in malonic and citric acid solutions as calculated according to four parameterization methods – black: Berkemeier (for malonic acid); teal: Laguerie; red: Reid; green: Lienhard; blue: Berkemeier; see text for details. Calculated values for a RH range between 10 and 90 % can be found in Table S2 of the Supplement.

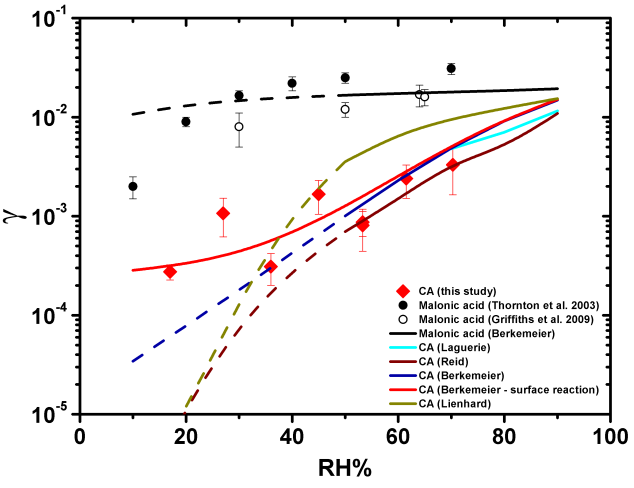

Figure 5. Parameterization of N_2O_5 uptake on citric acid aerosol according to Eq. (4) (lines) based on diffusivities estimated by the four parameterization methods: teal: Laguerie; dark red: Reid; green: Lienhard; blue: Berkemeier. Dashed lines indicate the RH range where the Stokes–Einstein relation (Eq. 7) is not strictly applicable. The red line represents the extended parameterization including a surface reaction term (Eq. 8), based on the Berkemeier H_2O diffusivity estimates. The black line represents the parameterization for malonic acid using the same kinetic parameters and diffusivity data estimated using the Berkemeier method for malonic acid; red diamonds: uptake coefficients measured in this study; solid circles: uptake coefficients for malonic acid according to Thornton et al. (2003); open circles: uptake coefficients for malonic acid according to Griffiths et al. (2009).

for diffusivity estimation. Figure 5 also shows data for liquid (supersaturated) malonic acid particles (Griffiths et al., 2009; Thornton et al., 2003) and the calculated uptake coefficient based on Eq. (4), using the corresponding estimate of N_2O_5 diffusivity. Thornton et al. (2003) have reported malonic acid efflorescence to occur at < 7 % RH and deliquescence at 69 % RH, and have performed experiments on solid malonic acid particles for comparison, which are not included here.

The parameterization based on the Lienhard et al. H_2O diffusivity data starts to deviate strongly from the rest as well as from the measured citric acid uptake coefficients above 30 % RH, overestimating the uptake by about a factor of 3–4. We note that the Vignes-type parameterization used by Lienhard et al. (2014) was constrained by measurements of the diffusivity of water below 40 % RH only at max. 281 K. Since H_2O is much smaller than N_2O_5, the diffusivity of N_2O_5 may exhibit a different slope as a function of humidity. The parameterization based on the Laguerie viscosity data is limited by the small range of solution compositions covered by measurements (RH > 70 %). The other parameterizations (Berkemeier, Reid) follow the measured values for the uptake coefficient fairly well down to about 50 % RH, indicating that the changing viscosity and associated changes in diffusivity as a function of RH control the uptake coefficient of N_2O_5. At lower RH the measured data seem to level off, which may be related to the decoupling between viscosity and diffusivity below 10 Pa s (Debenedetti and Stillinger, 2001; Power et al., 2013). However, this decoupling would rather lead to lower diffusivity of N_2O_5 than expected based on the Stokes–Einstein equation and thus fails to explain the higher than expected reactivity at low RH.

In spite of the uncertainties related to the diffusivity estimates, the uptake coefficient parameterized by Eq. (4), while well describing the measurements at higher RH, thus clearly underestimates the measurements at low RH. To assess the validity of the reacto-diffusive regime, we consider the reacto-diffusive length (Table 1), which remains much smaller than the particle dimensions, especially towards low humidity, due to the strong reduction in diffusivity. Thus no size effects are expected. In turn, Eq. (4) assumes that water, the reactant for N_2O_5, remains well mixed. Even for 15 % RH, using the diffusivity parameterization closest to our measured results (Berkemeier), the diffusivity of H_2O is about 1.34×10^{-10} cm^2 s^{-1}, and the characteristic time for diffusion across a particle, $t = d_p^2/D_{H2O}$, becomes about 0.75 s, which is significantly shorter than the residence time in the flow tube. Other effects, such as salting in of N_2O_5 (thus effectively increasing H) or an increase in the apparent rate constant k^{II} are also not likely. Therefore, we suggest that at low RH, uptake of N_2O_5 becomes limited by its hydrolysis on the surface, which is not included in Eq. (4). Including a surface reaction term to the uptake model would lead to

Table 1. Reacto-diffusive lengths calculated using diffusivity values obtained via the four above mentioned parameterizations.

	Reacto-diffusive length (nm)			
RH [%]	Laguerie	Reid	Berkemeier	Lienhard
30	–	0.09	0.21	0.16
50	–	0.49	0.74	2.88
70	3.03	1.83	2.96	7.21
90	6.33	5.26	9.63	10.29

$$\frac{1}{\gamma} = \frac{1}{\alpha_s} + \frac{1}{\Gamma_s + \left(\frac{1}{\Gamma_{sb}} + \frac{1}{\Gamma_b}\right)^{-1}}, \quad (8)$$

where α_s is the surface accommodation coefficient, and $1/\Gamma_{sb}$ represents the resistance for surface to bulk transfer (Ammann et al., 2013), which together constitute the bulk accommodation coefficient $1/\alpha_b = 1/\alpha_s + 1/\Gamma_{sb}$. The value of Γ_{sb} has been estimated by assuming that surface accommodation is not rate limiting and setting α_s to 1 and keeping α_b at 0.035 as above. Γ_s is the limiting uptake coefficient for the surface reaction. $1/\Gamma_b$ represents the bulk reaction-diffusion resistance given in Eq. (4).

The red line in Fig. 5 represents the result of applying Eq. (8), keeping the bulk reactivity parameters as before for the Berkemeier diffusivity estimates for citric acid and setting the value of Γ_s to 2.5×10^{-4}, which leads to good agreement with the observed data. The value of Γ_s falls into the range of uptake coefficients observed on effloresced malonic, succinic or oxalic acids (Griffiths et al., 2009; Thornton et al., 2003). Even at low RH, adsorbed water is abundant on a polar surface like citric acid, so that surface hydrolysis of N_2O_5 on high viscosity citric acid may indeed become the rate limiting step at low RH.

4 Conclusions and atmospheric impact

We have conducted measurements of N_2O_5 uptake to citric acid aerosol over an atmospherically relevant RH range at room temperature. Our results have shown that uptake coefficients change by roughly 1 order of magnitude ($\sim 3 \times 10^{-4}$–3×10^{-3}) between low (17 %) and high (70 %) RH. The results can be described under the assumption that citric acid remains a supersaturated liquid, even at low RH, and exhibits an increased viscosity at low water content. Reactive uptake is found to be governed by reacto-diffusive limitation with the reacto-diffusive length decreasing under the influence of increased viscosity (and thus decreased diffusivity) from a few nm to the sub-nanometer range. Thus, the decreasing uptake coefficients with decreasing RH are well explained by the parameterization of N_2O_5 uptake by the bulk reacto-diffusive uptake regime at RH above 50 %, essentially driven

by the decreasing diffusivity of N_2O_5. At low RH, estimating the diffusivity of N_2O_5 from the measured diffusivity of H_2O or the measured viscosity is problematic due to the decoupling between viscosity and diffusivity at high viscosity. However, even when taking these uncertainties into account, the reactivity observed at low RH cannot be explained by reaction in the bulk of the particles. We conclude that surface hydrolysis dominates uptake at low relative humidity.

Secondary organic aerosol (SOA) is likely to exhibit a similar, or even higher viscosity compared to citric acid used here as model compound (Renbaum-Wolff et al., 2013). Thus high viscosity at low RH could explain the discrepancy between N_2O_5 reactivity in field measurements and model predictions based on laboratory measurements. A recent study (Gaston et al., 2014) suggested that the organic O : C ratio in mixed inorganic-organic aerosols may be used as an indicator of N_2O_5 reactivity, based on a trend of increasing uptake coefficient with increasing O : C ratio. However, citric acid and some high O : C mixtures containing citric acid and other highly functionalized oxidized organic compounds were an exception to this trend. Hence, while O : C ratio can serve as an indicator for reactivity towards N_2O_5 at low O : C, this trend might be reversed for highly oxidized organic compounds forming high viscosity aqueous solutions. Parameterization of N_2O_5 reactivity in atmospheric models should thus not only rely on particle O : C, but should also have means to take into account high particle viscosity.

The Supplement related to this article is available online at doi:10.5194/acp-15-13615-2015-supplement.

Acknowledgements. The authors would like to thank the staff of the PSI accelerator facilities and of the isotope production facility IP-2 for their invaluable help. Additionally, the authors would like to thank C. Cai and J. Reid for supplying data on viscosity of citric acid. This work was supported by the Swiss National Science Foundation (grants no. 130175 and 149492). T. Berkemeier was supported by the Max Planck Graduate Center with the Johannes Gutenberg-Universität Mainz (MPGC) and thanks T. Koop for stimulating discussions.

Edited by: T. Bertram

References

Abbatt, J. P. D., Lee, A. K. Y., and Thornton, J. A.: Quantifying trace gas uptake to tropospheric aerosol: recent advances and remaining challenges, Chem. Soc. Rev., 41, 6555–6581, 2012.

Ammann, M.: Using ^{13}N as tracer in heterogeneous atmospheric chemistry experiments, Radiochim. Acta, 89, 831–838, 2001.

Ammann, M., Cox, R. A., Crowley, J. N., Jenkin, M. E., Mellouki, A., Rossi, M. J., Troe, J., and Wallington, T. J.: Evaluated kinetic and photochemical data for atmospheric chemistry: Volume VI – heterogeneous reactions with liquid substrates, Atmos. Chem. Phys., 13, 8045–8228, doi:10.5194/acp-13-8045-2013, 2013.

Anttila, T., Kiendler-Scharr, A., Tillmann, R., and Mentel, T. F.: On the reactive uptake of gaseous compounds by organic-coated aqueous aerosols: Theoretical analysis and application to the heterogeneous hydrolysis of N_2O_5, J. Phys. Chem. A, 110, 10435–10443, 2006.

Badger, C. L., Griffiths, P. T., George, I., Abbatt, J. P. D., and Cox, R. A.: Reactive uptake of N_2O_5 by aerosol particles containing mixtures of humic acid and ammonium sulfate, J. Phys. Chem. A, 110, 6986–6994, 2006.

Berkemeier, T., Shiraiwa, M., Pöschl, U., and Koop, T.: Competition between water uptake and ice nucleation by glassy organic aerosol particles, Atmos. Chem. Phys., 14, 12513–12531, doi:10.5194/acp-14-12513-2014, 2014.

Bertram, T. H. and Thornton, J. A.: Toward a general parameterization of N_2O_5 reactivity on aqueous particles: the competing effects of particle liquid water, nitrate and chloride, Atmos. Chem. Phys., 9, 8351–8363, doi:10.5194/acp-9-8351-2009, 2009.

Bertram, T. H., Thornton, J. A., Riedel, T. P., Middlebrook, A. M., Bahreini, R., Bates, T. S., Quinn, P. K., and Coffman, D. J.: Direct observations of N_2O_5 reactivity on ambient aerosol particles, Geophys. Res. Lett., 36, L19803, doi:10.1029/2009GL040248, 2009.

Brown, S. S., Dube, W. P., Fuchs, H., Ryerson, T. B., Wollny, A. G., Brock, C. A., Bahreini, R., Middlebrook, A. M., Neuman, J. A., Atlas, E., Roberts, J. M., Osthoff, H. D., Trainer, M., Fehsenfeld, F. C., and Ravishankara, A. R.: Reactive uptake coefficients for N_2O_5 determined from aircraft measurements during the Second Texas Air Quality Study: Comparison to current model parameterizations, J. Geophys. Res.-Atmos., 114, D00F10, doi:10.1029/2008JD011679, 2009.

Chang, W. L., Bhave, P. V., Brown, S. S., Riemer, N., Stutz, J., and Dabdub, D.: Heterogeneous Atmospheric Chemistry, Ambient Measurements, and Model Calculations of N_2O_5: A Review, Aerosol Sci. Technol., 45, 665–695, 2011.

Chmielewska, A. and Bald, A.: Viscosimetric studies of aqueous solutions of dicarboxylic acids, J. Mol. Liq., 137, 116–121, 2008.

Davidovits, P., Hu, J. H., Worsnop, D. R., Zahniser, M. S., and Kolb, C. E.: Entry of gas molecules into liquids, Faraday Discuss., 100, 65–81, 1995.

Davis, J. M., Bhave, P. V., and Foley, K. M.: Parameterization of N_2O_5 reaction probabilities on the surface of particles containing ammonium, sulfate, and nitrate, Atmos. Chem. Phys., 8, 5295–5311, doi:10.5194/acp-8-5295-2008, 2008.

Debenedetti, P. G. and Stillinger, F. H.: Supercooled liquids and the glass transition, Nature, 410, 259–267, 2001.

De Gouw, J. and Jimenez, J. L.: Organic Aerosols in the Earth's Atmosphere, Environ. Sci. Technol., 43, 7614–7618, 2009.

Dentener, F. J. and Crutzen, P. J.: Reaction of N_2O_5 on tropospheric aerosols: Impact on the global distributions of NO_x, O_3, and OH, J. Geophys. Res.-Atmos., 98, 7149–7163, doi:10.1029/92JD02979, 1993.

Gaston, C. J., Thornton, J. A., and Ng, N. L.: Reactive uptake of N_2O_5 to internally mixed inorganic and organic particles: the role of organic carbon oxidation state and inferred organic phase separations, Atmos. Chem. Phys., 14, 5693–5707, doi:10.5194/acp-14-5693-2014, 2014.

George, C., Ponche, J. L., Mirabel, P., Behnke, W., Scheer, V., and Zetzsch, C.: Study of the Uptake of N_2O_5 by Water and NaCl Solutions, J. Phys. Chem., 98, 8780–8784, 1994.

Griffiths, P. T., Badger, C. L., Cox, R. A., Folkers, M., Henk, H. H., and Mentel, T. F.: Reactive Uptake of N_2O_5 by Aerosols Containing Dicarboxylic Acids. Effect of Particle Phase, Composition, and Nitrate Content, J. Phys. Chem. A, 113, 5082–5090, 2009.

Gross, S., Iannone, R., Xiao, S., and Bertram, A. K.: Reactive uptake studies of NO_3 and N_2O_5 on alkenoic acid, alkanoate, and polyalcohol substrates to probe nighttime aerosol chemistry, Phys. Chem. Chem. Phys., 11, 7792–7803, 2009.

Gržinić, G., Bartels-Rausch, T., Birrer, M., Türler, A., and Ammann, M.: Production and use of ^{13}N labeled N_2O_5 to determine gas–aerosol interaction kinetics, Radiochim. Acta, 102, 1025–1034, 2014.

Guimbaud, C., Arens, F., Gutzwiller, L., Gäggeler, H. W., and Ammann, M.: Uptake of HNO_3 to deliquescent sea-salt particles: a study using the short-lived radioactive isotope tracer ^{13}N, Atmos. Chem. Phys., 2, 249–257, doi:10.5194/acp-2-249-2002, 2002.

Hallquist, M., Stewart, D. J., Stephenson, S. K., and Cox, R. A.: Hydrolysis of N_2O_5 on sub-micron sulfate aerosols, Phys. Chem. Chem. Phys., 5, 3453–3463, 2003.

Hanson, D. R. and Ravishankara, A. R.: The reaction probabilities of $ClONO_2$ and N_2O_5 on 40 to 75 % sulfuric acid solutions, J. Geophys. Res.-Atmos., 96, 17307–17314, doi:10.1029/91JD01750, 1991.

Hu, J. H. and Abbatt, J. P. D.: Reaction probabilities for N_2O_5 hydrolysis on sulfuric acid and ammonium sulfate aerosols at room temperature, J. Phys. Chem. A, 101, 871–878, 1997.

Kalberer, M., Tabor, K., Ammann, M., Parrat, Y., Weingartner, E., Piguet, D., Rössler, E., Jost, D. T., Türler, A., Gäggeler, H. W., and Baltensperger, U.: Heterogeneous chemical processing of (NO_2)-N-13 by monodisperse carbon aerosols at very low concentrations, J. Phys. Chem., 100, 15487–15493, 1996.

Kanakidou, M., Seinfeld, J. H., Pandis, S. N., Barnes, I., Dentener, F. J., Facchini, M. C., Van Dingenen, R., Ervens, B., Nenes, A., Nielsen, C. J., Swietlicki, E., Putaud, J. P., Balkanski, Y., Fuzzi, S., Horth, J., Moortgat, G. K., Winterhalter, R., Myhre, C. E. L., Tsigaridis, K., Vignati, E., Stephanou, E. G., and Wilson, J.: Organic aerosol and global climate modelling: a review, Atmos. Chem. Phys., 5, 1053–1123, doi:10.5194/acp-5-1053-2005, 2005.

Karagulian, F., Santschi, C., and Rossi, M. J.: The heterogeneous chemical kinetics of N_2O_5 on $CaCO_3$ and other atmospheric mineral dust surrogates, Atmos. Chem. Phys., 6, 1373–1388, doi:10.5194/acp-6-1373-2006, 2006.

Koop, T., Bookhold, J., Shiraiwa, M., and Pöschl, U.: Glass transition and phase state of organic compounds: dependency on molecular properties and implications for secondary organic aerosols in the atmosphere, Phys. Chem. Chem. Phys., 13, 19238–19255, 2011.

Laguerie, C., Aubry, M., and Couderc, J. P.: Some physicochemical data on monohydrate citric acid solutions in water: solubility, density, viscosity, diffusivity, pH of standard solution, and refractive index, J. Chem. Eng. Data., 21, 85–87, 1976.

Laskin, A., Moffet, R. C., Gilles, M. K., Fast, J. D., Zaveri, R. A., Wang, B., Nigge, P., and Shutthanandan, J.: Tropospheric chemistry of internally mixed sea salt and organic particles: Surprising reactivity of NaCl with weak organic acids, J. Geophys. Res.-Atmos., 117, D15302, doi:10.1029/2012JD017743, 2012.

Lienhard, D. M., Bones, D. L., Zuend, A., Krieger, U. K., Reid, J. P., and Peter, T.: Measurements of Thermodynamic and Optical Properties of Selected Aqueous Organic and Organic–Inorganic Mixtures of Atmospheric Relevance, J. Phys. Chem. A, 116, 9954–9968, 2012.

Lienhard, D. M., Huisman, A. J., Bones, D. L., Te, Y.-F., Luo, B. P., Krieger, U. K., and Reid, J. P.: Retrieving the translational diffusion coefficient of water from experiments on single levitated aerosol droplets, Phys. Chem. Chem. Phys., 16, 16677–16683, 2014.

Mentel, T. F., Sohn, M., and Wahner, A.: Nitrate effect in the heterogeneous hydrolysis of dinitrogen pentoxide on aqueous aerosols, Phys. Chem. Chem. Phys., 1, 5451–5457, 1999.

Mikhailov, E., Vlasenko, S., Martin, S. T., Koop, T., and Pöschl, U.: Amorphous and crystalline aerosol particles interacting with water vapor: conceptual framework and experimental evidence for restructuring, phase transitions and kinetic limitations, Atmos. Chem. Phys., 9, 9491–9522, doi:10.5194/acp-9-9491-2009, 2009.

Mozurkewich, M. and Calvert, J. G.: Reaction probability of N_2O_5 on aqueous aerosols, J. Geophys. Res.-Atmos., 93, 15889–15896, doi:10.1029/JD093iD12p15889, 1988.

Murray, B. J.: Inhibition of ice crystallisation in highly viscous aqueous organic acid droplets, Atmos. Chem. Phys., 8, 5423–5433, doi:10.5194/acp-8-5423-2008, 2008.

Peng, C., Chan, M. N., and Chan, C. K.: The hygroscopic properties of dicarboxylic and multifunctional acids: Measurements and UNIFAC predictions, Environ. Sci. Technol., 35, 4495–4501, 2001.

Power, R. M., Simpson, S. H., Reid, J. P., and Hudson, A. J.: The transition from liquid to solid-like behaviour in ultrahigh viscosity aerosol particles, Chemical Science, 4, 2597–2604, 2013.

Price, H. C., Murray, B. J., Mattsson, J., O'Sullivan, D., Wilson, T. W., Baustian, K. J., and Benning, L. G.: Quantifying water diffusion in high-viscosity and glassy aqueous solutions using a Raman isotope tracer method, Atmos. Chem. Phys., 14, 3817–3830, doi:10.5194/acp-14-3817-2014, 2014.

Renbaum-Wolff, L., Grayson, J. W., Bateman, A. P., Kuwata, M., Sellier, M., Murray, B. J., Shilling, J. E., Martin, S. T., and Bertram, A. K.: Viscosity of α-pinene secondary organic material and implications for particle growth and reactivity, P. Natl. Acad. Sci. USA, 110, 8014–8019, 2013.

Riemer, N., Vogel, H., Vogel, B., Anttila, T., Kiendler-Scharr, A., and Mentel, T. F.: Relative importance of organic coatings for the heterogeneous hydrolysis of N_2O_5 during summer in Europe, J. Geophys. Res.-Atmos., 114, D17307, doi:10.1029/2008JD011369, 2009.

Robinson, G. N., Worsnop, D. R., Jayne, J. T., Kolb, C. E., and Davidovits, P.: Heterogeneous uptake of $ClONO_2$ and N_2O_5 by sulfuric acid solutions, J. Geophys. Res.-Atmos., 102, 3583–3601, doi:10.1029/96JD03457, 1997.

Shiraiwa, M., Yee, L. D., Schilling, K. A., Loza, C. L., Craven, J. S., Zuend, A., Ziemann, P. J., and Seinfeld, J. H.: Size distribution dynamics reveal particle-phase chemistry in organic aerosol formation, P. Natl. Acad. Sci. USA, 110, 11746–11750, 2013.

Sosedova, Y., Rouvière, A., Gäggeler, H. W., and Ammann, M.: Uptake of NO_2 to Deliquesced Dihydroxybenzoate Aerosol Particles, J. Phys. Chem. A, 10979–10987, 2009.

Thornton, J. A. and Abbatt, J. P. D.: N_2O_5 reaction on submicron sea salt aerosol: Kinetics, products, and the effect of surface active organics, J. Phys. Chem. A, 109, 10004–10012, 2005.

Thornton, J. A., Braban, C. F., and Abbatt, J. P. D.: N_2O_5 hydrolysis on sub-micron organic aerosols: the effect of relative humidity, particle phase, and particle size, Phys. Chem. Chem. Phys., 5, 4593–4603, 2003.

Vaden, T. D., Imre, D., Beránek, J., Shrivastava, M., and Zelenyuk, A.: Evaporation kinetics and phase of laboratory and ambient secondary organic aerosol, P. Natl. Acad. Sci. USA, 108, 2190–2195, 2011.

Vandoren, J. M., Watson, L. R., Davidovits, P., Worsnop, D. R., Zahniser, M. S., and Kolb, C. E.: Uptake of N_2O_5 and HNO_3 by Aqueous Sulfuric-Acid Droplets, J. Phys. Chem., 95, 1684–1689, 1991.

Virtanen, A., Joutsensaari, J., Koop, T., Kannosto, J., Yli-Pirila, P., Leskinen, J., Makela, J. M., Holopainen, J. K., Pöschl, U., Kulmala, M., Worsnop, D. R., and Laaksonen, A.: An amorphous solid state of biogenic secondary organic aerosol particles, Nature, 467, 824–827, 2010.

Vlasenko, A., Huthwelker, T., Gäggeler, H. W., and Ammann, M.: Kinetics of the heterogeneous reaction of nitric acid with mineral dust particles: an aerosol flowtube study, Phys. Chem. Chem. Phys., 11, 7921–7930, 2009.

Wahner, A., Mentel, T. F., Sohn, M., and Stier, J.: Heterogeneous reaction of N_2O_5 on sodium nitrate aerosol, J. Geophys. Res.-Atmos., 103, 31103–31112, doi:10.1029/1998JD100022, 1998.

Zardini, A. A., Sjogren, S., Marcolli, C., Krieger, U. K., Gysel, M., Weingartner, E., Baltensperger, U., and Peter, T.: A combined particle trap/HTDMA hygroscopicity study of mixed inorganic/organic aerosol particles, Atmos. Chem. Phys., 8, 5589–5601, doi:10.5194/acp-8-5589-2008, 2008.

Zhang, Q., Jimenez, J. L., Canagaratna, M. R., Allan, J. D., Coe, H., Ulbrich, I., Alfarra, M. R., Takami, A., Middlebrook, A. M., Sun, Y. L., Dzepina, K., Dunlea, E., Docherty, K., DeCarlo, P. F., Salcedo, D., Onasch, T., Jayne, J. T., Miyoshi, T., Shimono, A., Hatakeyama, S., Takegawa, N., Kondo, Y., Schneider, J., Drewnick, F., Borrmann, S., Weimer, S., Demerjian, K., Williams, P., Bower, K., Bahreini, R., Cottrell, L., Griffin, R. J., Rautiainen, J., Sun, J. Y., Zhang, Y. M., and Worsnop, D. R.: Ubiquity and dominance of oxygenated species in organic aerosols in anthropogenically-influenced Northern Hemisphere midlatitudes, Geophys. Res. Lett., 34, L13801, doi:10.1029/2007GL029979, 2007.

Zobrist, B., Marcolli, C., Pedernera, D. A., and Koop, T.: Do atmospheric aerosols form glasses?, Atmos. Chem. Phys., 8, 5221–5244, doi:10.5194/acp-8-5221-2008, 2008.

Zobrist, B., Soonsin, V., Luo, B. P., Krieger, U. K., Marcolli, C., Peter, T., and Koop, T.: Ultra-slow water diffusion in aqueous sucrose glasses, Phys. Chem. Chem. Phys., 13, 3514–3526, 2011.